

# Magnetic properties of exchange biased and of unbiased oxide/permalloy thin layers: a ferromagnetic resonance and Brillouin scattering study

Fatih Zighem, Yves Roussigné, Salim Mourad Chérif and Philippe Moch  
*Laboratoire des Propriétés Mécaniques et Thermodynamiques des Matériaux,  
 CNRS UPR 9001, Université Paris Nord, 93430 Villetaneuse, France*

Jamal Ben Youssef  
*Laboratoire de Magnétisme de Bretagne, CNRS/FRE 3117,  
 Université de Bretagne Occidentale, 29285 Brest, France*

Fabien Paumier  
*Institut Pprime, CNRS UPR 3346, Université de Poitiers,  
 SP2MI-BP 30179, 86962 Chasseneuil-Futuroscope, France*

Microstrip ferromagnetic resonance and Brillouin scattering are used to provide a comparative determination of the magnetic parameters of thin permalloy layers interfaced with a non-magnetic ( $\text{Al}_2\text{O}_3$ ) or with an antiferromagnetic oxide (NiO). It is shown that the perpendicular anisotropy is monitored by an interfacial surface energy term which is practically independent of the nature of the interface. In the investigated interval of thicknesses (5-25 nm) the saturation magnetisation does not significantly differ from the reported one in bulk permalloy. In-plane uniaxial anisotropy and exchange-bias anisotropy are also derived from this study of the dynamic magnetic excitations and compared to our independent evaluations using conventional magnetometry

PACS numbers:  
 Keywords:

## I. INTRODUCTION

In magnetically ordered solids, the magnetic properties near a surface or an interface may differ in many respects from the observed one inside the bulk [1–3]. These differences are attributed to the reduced symmetry, to the lower coordination number and to the availability and role of highly localised surface and interface states inducing modified magnetic structures, sources of interesting magnetic behaviours. These phenomena which are generally localised within a few atomic layers are phenomenologically treated by means of surface anisotropies which provoke spin rearrangements inside thin magnetic films [2]. This paper focuses on metallic permalloy/oxide interfaces, comparing the cases of a nonmagnetic oxide ( $\text{Al}_2\text{O}_3$ ) with the case of an antiferromagnetic one (NiO). In this last situation, various interfacial effects have been put in evidence previously, such as hysteresis loop shifts and increased coercivity [4], training effects [4, 5] and rotatable anisotropy [7]. In particular, the so called exchange bias field was discovered nearly 50 years ago [4] and has given rise to a large number of experimental and theoretical publications [5–10]. Up to now, most of the experimental studies are based on hysteretic measurements and interpreted in terms of exchange bias ( $H_j$ ) and coercive ( $H_c$ ) fields. In contrast, only few ferromagnetic resonance (FMR) and Brillouin light scattering (BLS) studies, analysing the dynamic magnetic properties of exchange biased bilayers, are available [7, 10–16]. The present paper takes advantage of both techniques (more explicitly; retro-BLS and microstrip(MS)-FMR in view of interpreting this dynamics in interfaced poly-

crystalline  $\text{Ni}_{81}\text{Fe}_{19}$  thin films of various thicknesses. In addition, a careful examination of the interfaces was performed through high resolution electronic transmission microscopy (HRTEM) using a JEOL 3010 microscope (300 kV, LaB6, 0.19 nm point resolution).

The paper is organized as follows: in Section 2, we briefly describe the model used for the interpretation of the experimental data. Section 3 presents the two above cited techniques: BLS and MS-FMR. The experimental results are analysed and discussed in Section 4.

## II. THEORETICAL BACKGROUND

For an uncoupled permalloy layer, the volume magnetic energy density is written as:

$$\varepsilon_0 = \varepsilon_{zee.} + \varepsilon_{dip.} + \varepsilon_{exch.} + \varepsilon_{anis.} \quad (1)$$

where the first three terms stand for the Zeeman, the dipolar and the exchange contributions, respectively. The last term represents the anisotropy contribution and can be expressed as [1–3]:

$$\varepsilon_{anis.} = -\frac{(\vec{M} \cdot \vec{n})^2}{M^2} K_{\perp} - \frac{(\vec{M} \cdot \vec{u})^2}{M^2} K_u \quad (2)$$

In equation (2),  $\vec{M}$  is the magnetisation. The unit vector  $\vec{n}$  is normal to the film and consequently,  $K_{\perp}$  represents a uniaxial perpendicular anisotropy parameter. In addition,  $\vec{u}$  is an in-plane unit vector and  $K_u$

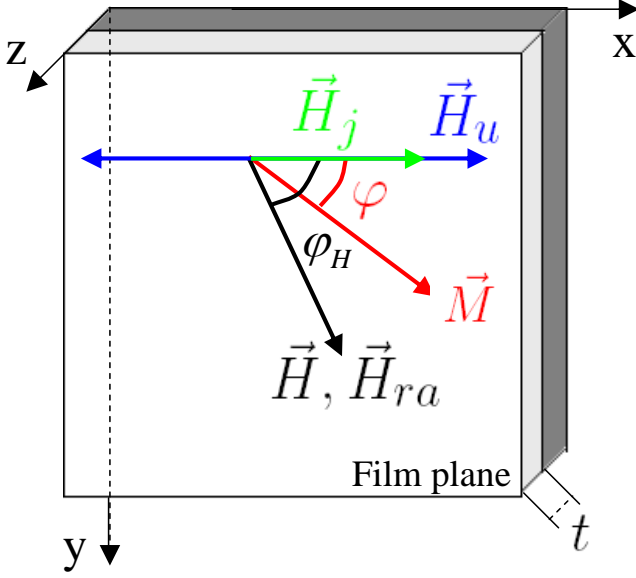


Figure 1: Sketch of the coordinate system used with the assumption that  $\theta = \pi/2$ . In the experiments presented here, the magnetic field is applied in the  $(xy)$  plane. Note that  $\vec{H}_u$  and  $\vec{H}_j$  are parallel one to each other and aligned along  $\vec{e}_x$ .  $\vec{H}_{ra}$  stands to be roughly parallel to the in-plane applied magnetic field.

stands for an in-plane anisotropy parameter. In most cases,  $K_{\perp}$  consists in an effective uniaxial anisotropy parameter which results from the addition of a bulk (presumably magnetocrystalline) term and of a surface term which depends on the film thickness  $t$ :

$$K_{\perp} = K_{\perp B} + \frac{K_{\perp S}}{t} \quad (3)$$

The bulk term value was previously found to lie around  $10^5 \text{ erg.cm}^{-3}$  [17]: as discussed in section 4 it is negligible compared to the experimental determination of  $K_{\perp}$ . A similar partition (bulk + surface) could be done for the in-plane anisotropy, but, as shown in section IV, does not provide for useful conclusions.

We define, as usual, the uniaxial perpendicular and the uniaxial in-plane anisotropy fields  $H_{\perp}$  and  $H_u$ , respectively, as:

$$H_{\perp} = \frac{2K_{\perp}}{M} ; H_u = \frac{2K_u}{M} \quad (4)$$

When the permalloy layer is interfaced with an anti-ferromagnetic layer, the magnetic energy density includes an additional contribution  $\varepsilon_b$  [7]:

$$\varepsilon_b = -\frac{\vec{M} \cdot \vec{v}}{M} j - \frac{\vec{M} \cdot \vec{H}}{MH} j_{ra} \quad (5)$$

In equation (5),  $j$  and the in-plane vector  $\vec{v}$  allow for defining the unidirectional anisotropy. It is usual to introduce the exchange bias field  $\vec{H}_j$ :

$$\vec{H}_j = \frac{j}{M} \vec{v} \quad (6)$$

The last term in equation (5) stands for a rotatable anisotropy [7]. It has not to be taken in consideration for determining the orientation of the magnetisation at equilibrium but it induces a so-called rotatable field  $\vec{H}_{ra}$  in the equation of motion monitoring the dynamics:

$$\vec{H}_{ra} = \frac{j_{ra}}{MH} \vec{H} \quad (7)$$

Generally,  $\varepsilon_b$  is considered as an effective volume density arising from a surface contribution depending of two parameters,  $j_S$  and  $j_{raS}$ : such an assumption provides  $j = j_S/t$  and  $j_{ra} = j_{raS}/t$ .

Figure 1 shows the above defined vectors and the used angular notations. In agreement with our experimental results discussed below we have taken  $\vec{u}$  parallel to  $\vec{v}$ : this provides simplifications which are not always satisfied [16, 18].

In the present work we specially focused on the uniform magnetic mode, the frequency  $f$  and the linewidth  $\Delta f$  of which were measured by MS-FMR. It results from the Landau-Lifshitz-Gilbert equation of motion that, for this mode,  $f$  and  $\Delta f$  are given by [19]:

$$\left(\frac{2\pi f}{\gamma}\right)^2 = \frac{1}{(M \sin \theta)^2} \left( \frac{\partial^2 \varepsilon}{\partial \theta^2} \frac{\partial^2 \varepsilon}{\partial \varphi^2} - \left( \frac{\partial^2 \varepsilon}{\partial \theta \partial \varphi} \right)^2 \right) \\ \frac{2\pi \Delta f}{\gamma} = \frac{\alpha}{M} \left( \frac{\partial^2 \varepsilon}{\partial \theta^2} - \frac{1}{\sin^2 \theta} \frac{\partial^2 \varepsilon}{\partial \varphi^2} \right) \quad (8)$$

In the above expressions  $\theta$  and  $\varphi$  stands for the polar angles of  $\vec{M}$ ,  $\alpha$  is the dimensionless Gilbert coefficient and  $\gamma$  is the effective gyromagnetic factor. For an in-plane applied field ( $\Rightarrow \theta = \pi/2$ ), one obtains:

$$\left(\frac{2\pi f}{\gamma}\right)^2 = H_1 \times H_2 \quad (9)$$

with

$$H_1 = ((H + H_{ra}) \cos(\varphi - \varphi_H) - H_u \cos 2\varphi + H_j \cos \varphi) \\ \text{and} \\ H_2 = ((H + H_{ra}) \cos(\varphi - \varphi_H) + H_{dem.} - H_{\perp} \\ + H_u \cos^2 \varphi + H_j \cos \varphi) \quad (10)$$

where  $H_{dem.} = 4\pi M$  is the demagnetizing field. The linewidth is given by:

$$\frac{2\pi \Delta f}{\gamma} = \alpha(2(H \cos(\varphi - \varphi_H) + H_u(3 \cos^2 \varphi - 1) + H_j \cos \varphi) + H_{dem.} - H_{\perp}) \quad (11)$$

In the case of low applied fields ( $H \ll H_{dem.eff.} = H_{dem.} - H_{\perp}$ ;  $H_{dem.eff.}$  is the effective demagnetizing field), the linewidth expression reduces to:

$$\left(\frac{2\pi f}{\gamma}\right)^2 = \alpha H_{dem.eff.} \quad (12)$$

In addition, the so-called DE mode [20] was studied by BLS. Its frequency depends on the wave vector  $\vec{q}$ . It is not given by an analytic expression but it can be numerically calculated [3]. However, for the  $qt$  values, small compared to unity, involved in our Brillouin study, an approximate analytic expression can be obtained [21, 22]. It is given by equation (9), with the following modified values of and :

$$H_1 = ((H + H_{ra}) \cos(\varphi - \varphi_H) + \frac{H_{dem.}}{1 + qt/2} - H_{\perp} + \frac{2A}{M} q^2 + H_u \cos^2 \varphi + H_j \cos \varphi) \quad \text{and}$$

$$H_2 = ((H + H_{ra}) \cos(\varphi - \varphi_H) + \frac{H_{dem.} \cos^2(\varphi - \varphi_H)}{1 + 2/qt} + \frac{2A}{M_s} q^2 + H_u \cos 2\varphi + H_j \cos \varphi) \quad (13)$$

$A$  is the exchange stiffness coefficient. Note that for  $q \rightarrow 0$ , we retrieve the expression of the uniform mode.

### III. EXPERIMENTAL SETUPS AND SAMPLES

#### A. Experimental setups

The measurements were performed at room temperature using both MS-FMR and BLS techniques. In MS-FMR the resonance is probed by sweeping the frequency of a pumping RF field  $h_{rf}$  in presence of a fixed applied magnetic field. More precisely, the amplitude of the applied magnetic field is subject to a slight modulation at low frequency ( $\sim 140$  Hz), thus allowing for a synchronous detection system. This technique gives access to the first derivative of the RF absorption versus the applied field. This absorption is generally described by a lorentzian function. The main advantage, compared to conventional FMR, consists in the availability of resonance studies with various

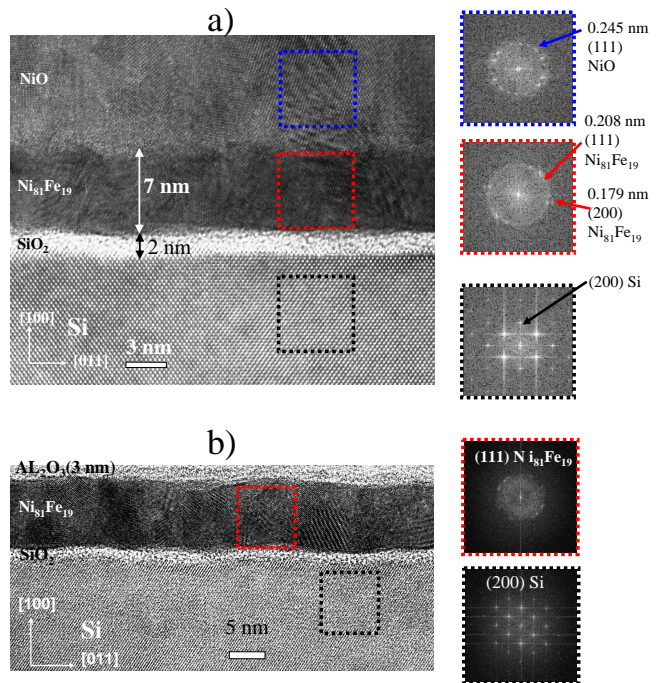


Figure 2: HRTEM images of the NiO/Ni<sub>81</sub>Fe<sub>19</sub> (a) and of the Al<sub>2</sub>O<sub>3</sub>/Ni<sub>81</sub>Fe<sub>19</sub> (b) interfaces. The colored squares on the right correspond to local Fourier transforms of the respectively colored areas of the picture.

amplitudes of the applied field and not only with various directions. Practically, the orders of magnitude of the in-plane anisotropy terms do not allow for their determination through conventional FMR while such determinations are easily performed using MS-FMR which is compatible with the necessarily low values of the applied magnetic fields. However, with MS-FMR, the rather large lack of spatial homogeneity of the RF field is a source of distortions of the absorption signal which prevent for very precise resonance frequency and linewidth evaluations [23, 24].

BLS was investigated in order to study the dispersion of the propagating magnetic mode versus the wave-vector  $\vec{q}$  (in the so-called Damon-Eschbach geometry, which designates geometrical arrangements characterized by a wave-vector normal to the magnetisation at equilibrium). The appropriately polarized spectra were studied in retro-scattering conditions using a  $3 \times 2$  tandem Fabry-Pérot interferometer illuminated by a single-mode Ar<sup>+</sup> ion laser at a wavelength of  $\Lambda = 514.5$  nm with a power of a few hundreds of mW. The sweeping of  $q$  was obtained by varying the angle of incidence of the optical beam ( $q = 4\pi \sin \psi / \Lambda$ , where  $\psi$  is the angle of incidence). In addition, some magnetic measurements were performed using a vibrating sample magnetometer (VSM), mainly in view of deriving coercive and bias fields from the observed magnetisation curves.

## B. Studied Samples

Two series of samples were elaborated using radio frequency sputtering on a silicon substrate covered by a thin (2 nm) SiO<sub>2</sub> layer. In the first one, the NiO thickness is fixed to 80 nm and the permalloy thickness  $t$  varies from 25 to 5 nm (25, 14, 9, 7.5, 6 and 5 nm). In the second one, the nickel oxide layer is replaced by a thin film (3 nm) of alumina (Al<sub>2</sub>O<sub>3</sub>) and the set of permalloy layers is unchanged : this second series defines a reference in order to evaluate the interfacial changes related to the antiferromagnetic/ferromagnetic boundary. High resolution transmission electron micrographs (HRTEM) were performed (see Figure 2) in view of getting information on the microstructure of each sub-layer in a given sample. The thicknesses are found in good agreement with the calculated ones from the deposition conditions. The NiO and the Ni<sub>81</sub>Fe<sub>19</sub> films are well crystallized and composed of small crystallites with sizes of a few nm<sup>3</sup>). The NiO layers present columns around 5 nm in diameter and 30 nm in length. Moreover, no preferential texture is favoured, as attested by our electron diffraction studies (not shown here). This signifies that the NiO interface corresponds to a mixed structure including compensated and uncompensated magnetic moments. Nevertheless, the roughness of the interface does not exceed 0.5 nm (see Figure 2). Note also that the two series were studied in the absence of a preliminary cooling from the Néel temperature under a magnetic field applied in view of increasing the exchange bias. However, during the deposition a small residual in-plane magnetic field of 5 Oe is applied along  $\vec{e}_x$ , as above mentioned: it favours the interfacial exchange coupling.

## IV. RESULTS AND DISCUSSION

### A. Unbiased Al<sub>2</sub>O<sub>3</sub>/permalloy films

For this reference series the contribution  $\varepsilon_b$ , expressed in equation (5), vanishes. The frequency and the linewidth of the uniform mode are expected to only depend on the gyromagnetic factor  $\gamma$ , of the magnetisation  $M$ , of the uniaxial perpendicular anisotropy ( $K_{\perp}$ ), of the uniaxial in-plane anisotropy ( $K_u$ ) and of the damping ( $\alpha$ ) coefficients (and, indeed, of the sample thickness  $t$ ). In principle the study of their variations versus the amplitude and the direction of an applied magnetic field allows for the evaluation of these magnetic parameters. However, due to the limitations of the available precision, the MS-FMR study is mainly efficient to give access to  $H_{dem.eff.}$ ,  $H_u$  and  $\alpha$ , assuming a given value of  $\gamma$  (we took  $1.844 \times 10^7 \text{ s}^{-1} \cdot \text{Oe}^{-1}$  in agreement with the expected value (2.1) of the effective  $g$  factor ( $\gamma = g \times 8.794 \times 10^6$ )).

The variations of the frequency versus the amplitude (see Figure 3) and the direction (see Figure 5) of an

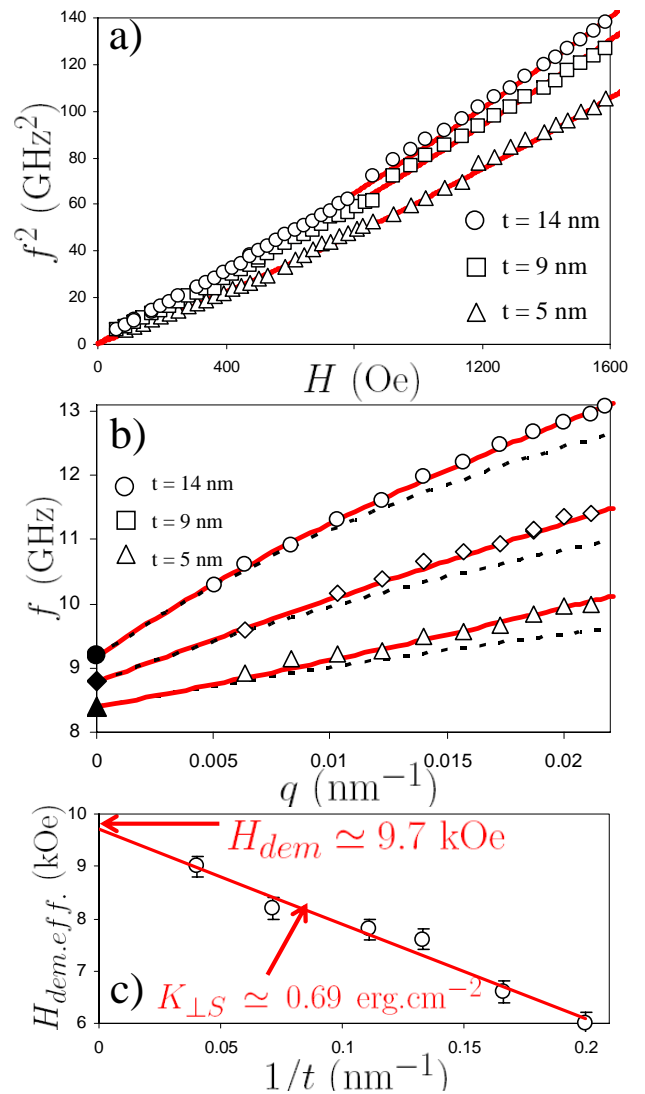


Figure 3: a) Squared resonance frequency versus the applied magnetic field along the easy axis ( $\vec{e}_x$  direction). b)  $q$ -dependence of the DE mode frequency for three characteristic thicknesses. Full lines correspond to the adjustments obtained by using equation 10 and 13. We have also reported the frequency of the uniform mode ( $q = 0$ ) measured by MS-FMR. The dashed lines correspond to the fit neglecting the exchange stiffness ( $A = 0$ ). c) Deduced  $H_{dem.eff.}$  values versus the inverse of the permalloy thickness: the found anisotropy constant value is  $K_{\perp S} \approx 0.69 \text{ erg.cm}^{-2}$ .

in-plane applied field were studied. It results from the analysis of the data that the surface coefficient  $2K_{\perp S}/M$  contributing to the perpendicular anisotropy does not depend on the studied sample. From its observed linear variation versus  $(1/t)$  we deduce a common value of the effective demagnetizing field at large thicknesses, equal to 9700 Oe (see Figure 3c). This value is very close to the reported one in bulk permalloy showing the same composition [25, 26]. As mentioned in section 2,  $2K_{\perp B}/M$  is not expected to exceed a few hundred Oe. With a rather

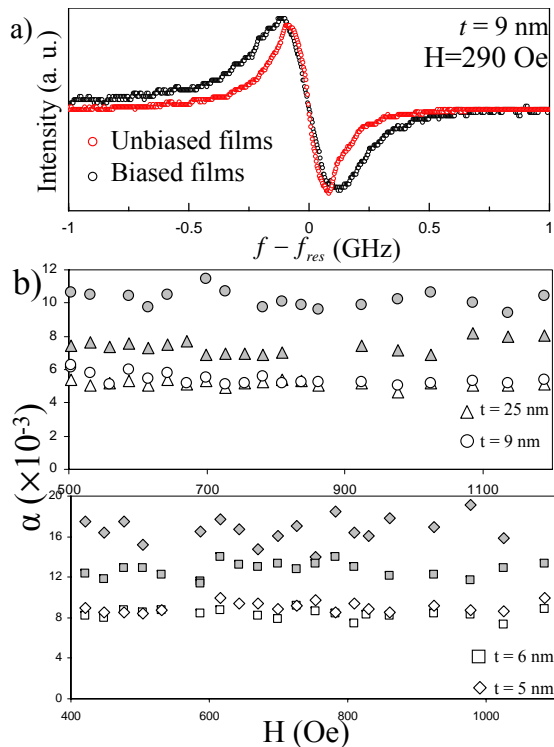


Figure 4: a) Typical spectra obtained from the two series of samples. Note the linewidth broadening obtained in presence of the nickel oxide layer. These examples correspond to spectra obtained from the samples of  $t = 9$  nm under an applied field of 290 Oe. For clarity, they are centered around 0 (shifted by their respective resonance frequency). b) Damping parameter  $\alpha$  versus the applied magnetic field. Open symbols represent unbiased films while filled symbols represent the results obtained from biased films.

good approximation, one can neglect this bulk anisotropy and conclude that, in the studied interval of thicknesses, all the samples show a saturation magnetisation practically equal to the measured one in the bulk material and are characterized by the same surface energy  $K_{\perp S} = 0.69$  erg.cm $^{-2}$ . Considering now the in-plane anisotropy, it is found very small, thus providing anisotropy fields of a few Gauss, with an easy axis parallel to the direction of the field induced during the elaboration process. In addition, the Gilbert damping model provides a satisfactory agreement of the observed linewidths: as expected from this model the deduced value of  $\alpha$  (see Figure 4b) does not depend on the applied field. It varies from one to another sample but always lies in the [0.005; 0.009] interval.

The anisotropy and magnetisation values calculated from the MS-FMR data provide a good fit of the Brillouin spectra: as written above, the  $q$  dependence of the frequency is deduced from its variation versus the angle of incidence of the illuminating beam. When its direction is nearly normal to the film this frequency practically does

not differ from the obtained one for the uniform mode, as illustrated on Figure 3b. For large  $q$  values the contribution of the exchange stiffness constant  $A$  is significant and has to be taken in account (see equation (13) and Figure 3b). For all the studied samples our measured value of  $A$  is equal to  $1 \times 10^{-6}$  erg.cm $^{-1}$ . However, this determination is rather approximate: to improve the precision it would be useful to observe the stationary magnetic modes [27] which, due to limitations in the available amplitude of the applied field, were not accessible in the present study. The complete set of the magnetic parameters deduced for the studied series of unbiased Al $_2$ O $_3$ /permalloy films is given in Table 1.

$t$ (nm)	$H_{dem.eff.}$ (kOe)	$H_u$ (Oe)	$\alpha$ $\times 10^{-3}$
25	9	$\sim 5$	5
14	8.2	$\sim 5$	6
9	7.8	$\sim 5$	5
7.5	7.6	$\sim 5$	7
6	6.6	$\sim 5$	9
5	6	$\sim 5$	8

$H_{dem.} = 9.7$  kOe;  $K_{\perp S} \simeq 0.69$  erg.cm $^{-2}$ ;  
 $A = 1 \times 10^{-6}$  erg.cm $^{-1}$

Table I: Unbiased Al $_2$ O $_3$ /permalloy films

## B. Biased NiO/permalloy films

The magnetisation curves, recorded with an in-plane applied magnetic field, clearly reveal an easy anisotropy axis and a bias field along the above mentioned residual magnetic field applied in  $\vec{e}_x$  direction during the deposition. Figure 5 shows examples of hysteresis graphs obtained along easy and hard directions. It also presents the variation versus  $\varphi_H$  of the remanent magnetisation after suppressing a saturating magnetic field inclined of  $\varphi_H$  from  $\vec{e}_x$ . The results can be interpreted in terms of a coherent uniform rotation model depending of an energy density containing both contributions of a coercive field ( $H_c$ ) and of a bias field ( $H_d$ ). The obtained values of ( $H_c$ ) and of ( $H_d$ ) are given in Table II. The MS-FMR measurements allow for evaluating the parameters enumerated in the previous section and, in addition, the bias and the rotatable fields appearing in such biased structures.

The first important result concerns the effective demagnetizing field: it practically does not differ from the measured one in the unbiased films described in the previous subsection. We then conclude to a perpendicular anisotropy coefficient mainly monitored by a surface term  $K_{\perp S}$ . We derive:  $K_{\perp S} = 0.65$  erg.cm $^{-2}$ , nearly the same value as in the unbiased samples (0.69 erg.cm $^{-2}$ ). Here again, the saturation magnetisation does not appreciably differ from the reported value in the bulk [25, 26]. The in-plane anisotropy parameters

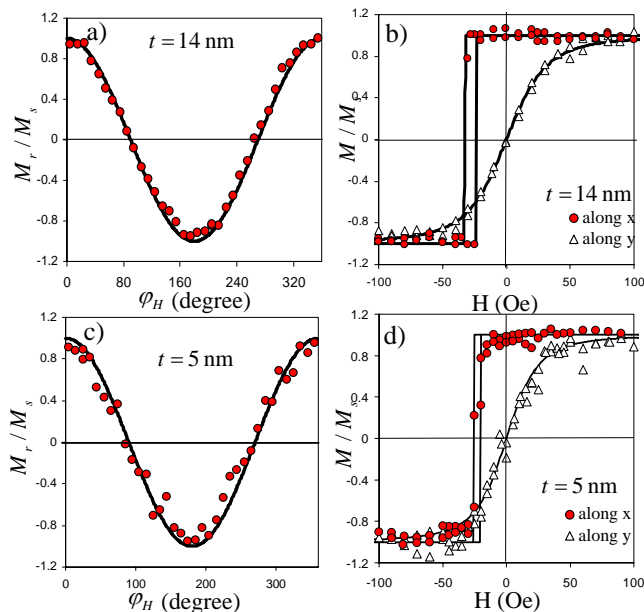


Figure 5: a) c) Angular dependence of the remanent magnetisation for two typical thicknesses (14 and 5 nm). Magnetisation curves measured at  $\varphi_H = 0^\circ$  (along  $\vec{e}_x$ ) and  $\varphi_H = 90^\circ$  (along  $\vec{e}_y$ ). The solid lines corresponds to the best fits obtained from the magnetic energy density presented in equation 1.

involved in these structures,  $H_u$ ,  $H_j$  and  $H_{ra}$ , are presented in Table II. Typical angular variations of the frequency versus the direction of the in-plane applied field, compared to the observed ones in unbiased samples of the same thickness, are shown on Figure 6. The uniaxial anisotropy field  $H_u$  does not overpass a few Oe, as it is the case in the unbiased samples. Notice that it does not significantly differ from the above discussed coercive field, as expected in the frame of a coherent uniform rotation model. A bias exchange field is observed in all the films: here again, it does not much differ from the static bias field  $H_d$  deduced from the hysteresis loops. In both cases there is no clear correlation between the in-plane anisotropy values and the thickness of the studied film. Table II also gives the Gilbert damping coefficients derived from the analysis of the linewidths of the studied resonances:  $\alpha$  is larger than in the unbiased layers and increases when the thickness decreases. This behaviour was pointed out in several publications [7, 15, 16]. A theoretical model introduced by Arias et al. [28] was adapted by Rezende et al. [29] in order to explain this broadening. In this model, it results from the lack of homogeneity of the interfacial exchange coupling between the ferromagnetic and antiferromagnetic layers and varies as  $t^{-2}$ . The magnetic parameters derived from our MS-FMR measurements are in agreement with the BLS results. The  $q$  dependence of the observed frequency is well accounted assuming an unchanged value of the exchange stiffness  $A$

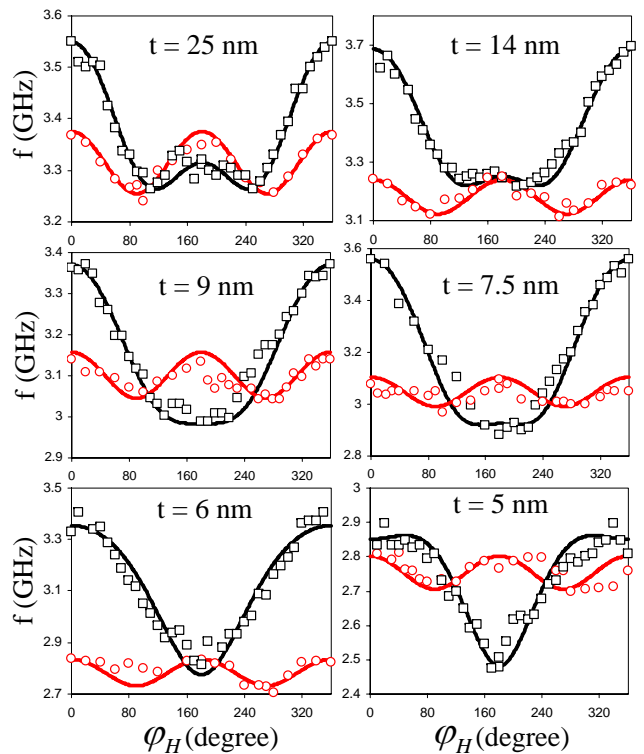


Figure 6: Angular dependence of the uniform mode frequency. A small in-plane applied magnetic field (140 Oe) was fixed to ensure the saturation magnetisation. The black squares correspond to the results obtained from the biased samples and the circles are the results obtained from the unbiased samples. The solid lines correspond to the best fits as calculated using equation 10. The different parameters used are presented on Table I and II.

( $1 \times 10^{-6}$  erg.cm $^{-1}$ ). However, due to the rather small in-plane anisotropy terms and to the limited available instrumental precision, their quantitative derivation through our BLS study is not very efficient.

$t$ (nm)	$H_{dem.eff.}$ (kOe)	$H_u$ (Oe)	$H_c$ (Oe)	$H_j$ (Oe)	$H_d$ (Oe)	$H_{ra}$ (Oe)	$\alpha_{app}(\times 10^{-3})$ —
25	9	6	5	10	10	0	7
14	8.4	8	5	20	23	15	9
9	7.6	4	4	18	30	8	10
7.5	7.3	3	8	32	41	18	14
6	7	3	5	27	24	15	12
5	5.1	2	3	21	28	25	16

$H_{dem.} = 9.7$  kOe;  $K_{\perp s} \simeq 0.65$  erg.cm $^{-2}$   
 $A = 1 \times 10^{-6}$  erg.cm $^{-1}$

Table II: Biased NiO/permalloy films

## V. CONCLUSION

Our comparative study of two series of permalloy ferromagnetic (F) layers covering a thickness interval extending from 5 to 25 nm, grown by RF sputtering, respectively on a non-magnetic oxide substrate ( $\text{Al}_2\text{O}_3$ ) and on an antiferromagnetic (AF) one (NiO), revealed expected differences originating from the exchange F/AF interfacial interaction but also some surprising similarities. In both cases the interface, observed by HRTEM, shows a very small roughness (below 0.5 nm). The dynamic magnetic properties put in evidence an uniaxial perpendicular anisotropy mainly originating from a contribution of the

surface density of energy which is practically independent of the nature of the interface ( $\text{Al}_2\text{O}_3$ /permalloy or NiO/permalloy). The saturation magnetisation does not vary versus the thickness and is close to the expected one in bulk permalloy showing the same composition. The in-plane anisotropy terms derived from MS-FMR data are in reasonable agreement with the deduced ones from conventional VSM magnetometry. The in-plane anisotropy field does not exceed a few Oe and is close to the coercive field ; its value is not clearly correlated neither to the thickness nor to the nature of the interface. The bias exchange is only observed in presence of a AF/F interface, as usual.

- 
- [1] L. Néel, *J. Phys. Radium* **15**, 225 (1954)
  - [2] C. Chappert and P. Bruno, *J. Appl. Phys.* **64**, 5736 (1988)
  - [3] Y. Roussigné, F. Ganot, C. Dugautier and D. Renard, *Phys. Rev. B* **52**, 350 (1995)
  - [4] W. H. Meiklejohn and C. P. Bean, *Phys. Rev.* **102**, 1413 (1956)
  - [5] J. Nogues, I. K. Schuller, *J. Magn. Magn. Mater.* **192**, 203 (1999)
  - [6] C. Binek, *Phys. Rev. B* **70**, 014421 (2004)
  - [7] R. D. McMichael, M. D. Stiles, P. J. Chen and W. F. Egelhoff, *Phys. Rev. B* **58**, 8605 (1998)
  - [8] J. Nogués, J. Sort, V. Langlais, V. Skumryev, S. Suriñach, J.S. Muñoz, M.D. Baró, *Physics Reports* **422**, 65 (2005).
  - [9] A.E. Berkowitz and K. Takano, *J. Magn. Magn. Mater.* **200**, 552 (1999).
  - [10] R. L. Stamps, *J. Phys. D: Appl. Phys.* **33**, R247 (2000)
  - [11] W. Stoeklein, S. S. P. Parkin and J. C. Scott, *Phys. Rev. B* **38**, 6847 (1988)
  - [12] J. Geshev, L. G. Pereira, J. E. Schmidt, L. C. C. M. Nagamine, E. B. Saitovitch and F. Pelegrini, *Phys. Rev. B* **67**, 132401 (1998)
  - [13] T. Blachowicz, *J. Appl. Phys.* **102**, 043901 (2007)
  - [14] L. Wee, R. L. Stamps, L. Malkinski and Z. Celinski, *Phys. Rev. B* **69**, 043901 (2007)
  - [15] S. M. Rezende, M. A. Lucena, A. Azevedo, F. M. de Aguiar, J. R. Fermin and S. S. P. Parkin, *J. Appl. Phys.* **93**, 7714 (2003)
  - [16] F. Zighem, Y. Roussigné, S.-M. Chérif and P. Moch, *J. Phys. Cond. Matter*, **20**, 125201 (2008)
  - [17] J. Ben Youssef, N. Vukadinovic, D. Billet and M. Labrune *Phys. Rev. B* **69**, 174402 (2004)
  - [18] M. O. Liedke, B. Liedke, A. Keller, B. Hillebrands, A. Mücklich, S. Fasco and J. Fassbender, *Phys. Rev. B*, **75**, 220407 (2007)
  - [19] U. Netzelmann, *J. Appl. Phys.* **68**, 1800 (1990)
  - [20] W. Damon and J. R. Eshbach *J. Phys. Chem. Solids*, **19**, 308 (1961)
  - [21] F. Zighem, Y. Roussigné, S.-M. Chérif and P. Moch, *J. Phys. Cond. Matter*, **19**, 176220 (2007)
  - [22] R. L. Stamps *Phys. Rev. B*, **49**, 339 (1994)
  - [23] G. Counil, J.-V. Kim, T. Devolder, P. Crozat, C. Chappert, K. Shigeto and Y. Otani *J. Appl. Phys.* **95**, 5646 (2004)
  - [24] G. Counil, J.-V. Kim, T. Devolder, C. Chappert and A. Cebollada *J. Appl. Phys.* **98**, 023901 (2005)
  - [25] G. I. Lykken, W. L. Harman and E. N. Mitchell, *J. Appl. Phys.* **37**, 3353 (1966)
  - [26] J. O. Rantschler, P. J. Chen, A. S. Arrott, R. D. McMichael, W. F. Egelhoff, Jr. and B. B. Maranville, *J. Appl. Phys.* **97**, 10J113 (2005)
  - [27] M. Belmeguenai, F. Zighem, Y. Roussigné, S.-M. Chérif, P. Moch, K. Westerholt, G. Woltersdorf and G. Bayreuther, *Phys. Rev. B*, **79**, 024419 (2009)
  - [28] R. Arias and D. L. Mills, *Phys. Rev. B* **60**, 7395 (1999)
  - [29] S. M. Rezende, A. Azevedo, M. A. Lucena and F. M. de Aguiar, *Phys. Rev. B* **63**, 214418 (2001)